# Physical Interpretation of MIMO Transmissions

A. van Zelst
Eindhoven University of Technology, P.O. Box 513, 5600 MB Eindhoven,
the Netherlands, e-mail: A.v.Zelst@tue.nl,
and Agere Systems, P.O. Box 755, 3430 AT Nieuwegein, the Netherlands,
e-mail: Zelst@agere.com

***Abstract*—Information theoretical analysis has shown that the application of multiple antennas at both sides of the wireless communication link can greatly improve the capacity/throughput. Although many mathematical analyses are performed on such a system, generally referred to as a Multiple-Input Multiple-Output (MIMO) system, a physical interpretation of the MIMO principle is still lacking in literature. In this paper, a physical interpretation is presented by which it is shown that a given MIMO system is more robust in richly-scattered environments.**

## I. Introduction

Applying multiple antennas at both the transmitter and receiver side can, especially when the environment provides rich scattering, greatly improve the capacity/throughput of a wireless communication link in flat fading [1]. It has been shown by information theory that the capacity grows linearly with the number of eigenmodes of the wireless channel. The number of eigenmodes can be as large as the minimum of the number of transmit (TX) and receive (RX) antennas, provided that the channel coefficients from every TX to every RX antenna are independent and identically distributed. Besides various mathematical evaluations in which above considerations are worked out in depth, to the author's knowledge, the MIMO principle has never been explained by a physical interpretation. The goal of this paper is to provide such an explanation.

## II. Multiple-Input Multiple-Output Communication

Consider a wireless communication system with $N_t$ transmit (TX) and $N_r$ receive (RX) antennas. The idea is to transmit different streams of data on the different transmit antennas, but at the same carrier frequency. The stream on the $p$-th transmit antenna, as function of the time $t$, will be denoted by $s_p(t)$. When a transmission occurs, the transmitted signal from the $p$-th TX antenna might find different paths to arrive at the $q$-th RX antenna, namely, a direct path and indirect paths through a number of reflections. This principle is called *multipath*. Suppose that the bandwidth $B$ of the system is chosen such that the time delay between the first and last arriving path at the receiver is considerably smaller than $1/B$, then the system is called a *narrowband* system. For such a system, all the multipath components between the $p$-th TX and $q$-th RX antenna can be summed up to one term, say $h_{qp}(t)$. Since the signals from all transmit antennas are sent at the same frequency, the $q$-th receive antenna will not only receive signals from the $p$-th, but from all $N_t$ transmitters. This can be denoted by the following equation (the additive noise at the receiver is omitted for clarity)

$$x_q(t) = \sum_{p=1}^{N_t} h_{qp}(t) s_p(t), \tag{1}$$

To capture all $N_r$ received signals into one equation, the matrix notation can be used:

$$\mathbf{x}(t) = \mathbf{H}(t)\mathbf{s}(t), \tag{2}$$

where $\mathbf{s}(t)$ is an $N_t$-dimensional column vector with $s_p(t)$ being its $p$-th element, $\mathbf{x}(t)$ is $N_r$-dimensional with $x_q(t)$ on its $q$-th position and the matrix $\mathbf{H}(t)$ is $N_r \times N_t$ with $h_{qp}(t)$ as its $(q,p)$-th element, with $p = 1, \ldots, N_t$ and $q = 1, \ldots, N_r$. A schematic representation of a MIMO communication scheme can be found in Figure 1.

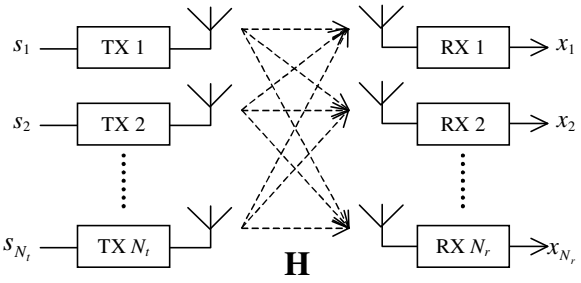


Figure 1: Schematic representation of a MIMO communication system.

Mathematically, a MIMO transmission can be seen as a set of equations (the recordings on each RX antenna) with a number of unknowns (the transmitted signals). If every equation represents a unique combination of the unknown variables and the number of equations is equal to the number of unknowns, then their exits a unique solution to the problem. If the number of equations is larger than the number of unknowns, a solution can be found by performing a pro-

This work is sponsored by Agere Systems, the Netherlands, and the Dutch cooperative research project B4 BroadbandRadio@Hand, BTS01063.

jection using the *least squares* method ([2]), also known as the *Zero Forcing* (ZF) method. For the symmetric case, the ZF solution results in the unique solution.

Suppose the coefficients of the unknowns are gathered in the channel matrix $\mathbf{H}(t)$ and the number of parallel transmit signals (unknown variables) equals to the number of received signals (equations), then the equations are solvable when $\mathbf{H}(t)$ is invertible. Under this condition, the solution of (2) can be found by multiplying both sides with the inverse of $\mathbf{H}(t)$:

$$\mathbf{H}^{-1}(t)\mathbf{x}(t) = \mathbf{H}^{-1}(t)\mathbf{H}(t)\mathbf{s}(t) = \mathbf{I}_{N_t}\mathbf{s}(t) = \mathbf{s}(t), \quad (3)$$

where $\mathbf{I}_N$ is the $N \times N$ dimensional identity matrix. To find the inverse of $\mathbf{H}(t)$, the channel matrix must be known at the receiver. This can be done by, e.g., sending a training sequence, that is known to the receiver, to train the channel.

In the next sections, a system with two transmit antennas ($N_t = 2$) and two receive antennas ($N_r = 2$), or shortly, a $2 \times 2$ system is considered. It will be assumed that the receiver perfectly knows the channel. With this assumption, we may write the two solutions $s_1(t)$ and $s_2(t)$ as

$$s_1(t) = \mathbf{w}^1(t)\mathbf{x}(t), \quad (4)$$

$$s_2(t) = \mathbf{w}^2(t)\mathbf{x}(t), \quad (5)$$

where the $\mathbf{w}^i(t)$ denotes the weight that is applied at the receiver to estimate the $i$-th transmitted signal and can be shown to be equal to the $i$-th row of $\mathbf{H}^{-1}(t)$. In the next sections, we are going to determine the channel coefficients and the weights, and show what the effect of the weights is on the antenna pattern in a pure Line-of-Sight (LOS), i.e. a free space, scenario and what the effect is in a scenario with two ideal reflecting planes. In the final paper, a number of other scenarios are evaluated as well as the effect of channel estimation errors.

## III. Free Space

A free-space scenario is considered in which a $2 \times 2$ system is placed in an (artificial) environment where no reflections occur. Both the antenna set-up and the environment are assumed static and, therefore, the channel coefficients are constant over time. Hence, the time index can be omitted. Since no reflections take place, the channel coefficient between the $p$-th TX antenna and the $q$-th RX antenna, $h_{qp}$, only consists of the direct path between these antennas. Denote the length of this path by $d_{qp}$, then both the power and phase of the channel coefficient are a function of $d_{qp}$. Since the system is operation in free space, the power at a distance $d_{qp}$ from the $p$-th transmitter is given by the Friis free space equation ([3]):

$$P_r(d_{qp}) = \frac{P_t G_t G_r \lambda^2}{(4\pi)^2 d_{qp}^2 L_s} \text{ Watts}, \quad (6)$$

where $P_t$ is the transmitted power per TX antenna, $G_t$ and $G_r$ are, respectively, the transmitter and receiver antenna gains, $L_s$ is the system loss factor not related to propagation and $\lambda$ is the wavelength in meters. In the next analysis, we will assume that there is no system loss ($L_s = 1$) and that unity gain antennas are used. The phase at distance $d_{qp}$ equals $-2\pi d_{qp}/\lambda$ rad, where $\lambda$ denotes the wavelength. This results in the following channel coefficient

$$h_{qp} = \sqrt{\frac{P_t \lambda^2}{(4\pi)^2 d_{qp}^2}} \exp\left(-j2\pi \frac{d_{qp}}{\lambda}\right). \quad (7)$$

Once all elements of the channel matrix $\mathbf{H}$ are known, the weights for the Zero Forcing MIMO processing can be determined. The weight vectors $\mathbf{w}^1$ and $\mathbf{w}^2$ are obtained as described in Section II. We want to see what the effect of these weights is. To that end, a dummy antenna is placed at a given two dimensional spot $(x,y)$ and the received vector as function of $(x,y)$ is determined: $\mathbf{x}(x,y)$. This vector is multiplied by the weights $\mathbf{w}^1$ and $\mathbf{w}^2$, respectively, and we now can, e.g., show what the power is of the resulting signals as function of $(x,y)$. These plots can be seen as the antenna patterns after applying the weights.

Here, this is worked out for an antenna set-up as depicted in Figure 2. Assume that the TX antennas and RX antennas are centered around the $y$-axis, with an antenna spacing of respectively $d_{TX} = 1\lambda$ and $d_{RX} = 1\lambda$, furthermore, assume that the distance between the transmitter array and receiver array equals $D = 100\lambda$, and that the power per TX antenna equals 0.035 Watts. Using (7), $\mathbf{H}$ and the weight vectors can be determined, successively.

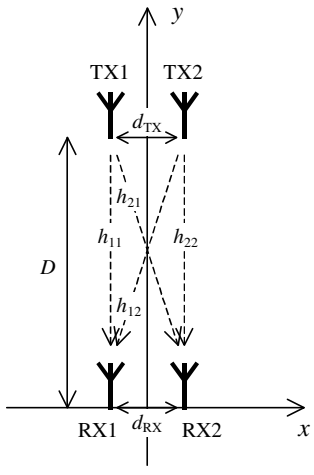


Figure 2: Antenna set-up.

Applying these weight vectors results in the antenna patterns as given in Figure 3. The points in the plots are calculated using a grid in polar coordinates, with an angular grid of $\frac{1}{2}\cdot\tan(\frac{1}{2}\cdot d_{TX}/D)\cdot 180/\pi \approx 0.143$ degrees and a radius grid of $1\lambda$. To smoothen the plots, interpolation is applied. Note that the TX antenna positions are denoted by the white crosses and the RX antenna positions by the black ones. We clearly see that, when weight $\mathbf{w}^1$ is used, the signal from the second antenna (and all spots in line with that TX antenna and the receiver array) is suppressed, and vice versa when $\mathbf{w}^2$ is applied. Clearly, the undesired signal is forced to zero. Furthermore, it can be seen that the larger the distance between a given spot $(x,y)$ and the receiver array, the weaker the signal that is received. This is a result of applying the free-space path loss model.

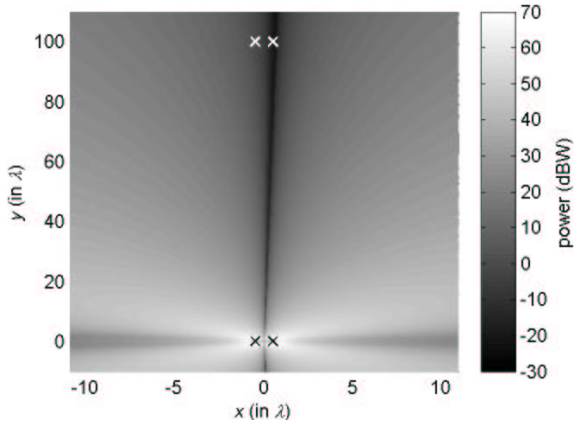


(a)

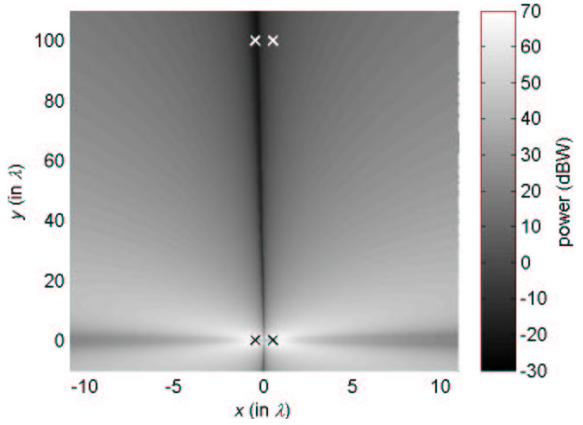


(b)

Figure 3: Antenna patterns after applying the first (a) and second (b) weight vector in free space.

## IV. One Reflecting Plane

Here, the scenario of the previous section is extended with one perfectly-reflecting plane, parallel to the transmitter-receiver line. In addition to the direct paths of the free-space case, one indirect path per channel element has to be taken into account due to the reflection. At the receiver side, this indirect path can be seen as if it would be a direct path from the *image* of the transmitter, mirrored in the reflecting plane (see Figure 4). So, for the channel between the $p$-th TX and the $q$-th RX antenna this means that, besides the direct path, an extra path must be added, virtually being the direct path from the image of the $p$-th TX antenna to the $q$-th receiver (see Figure 4).

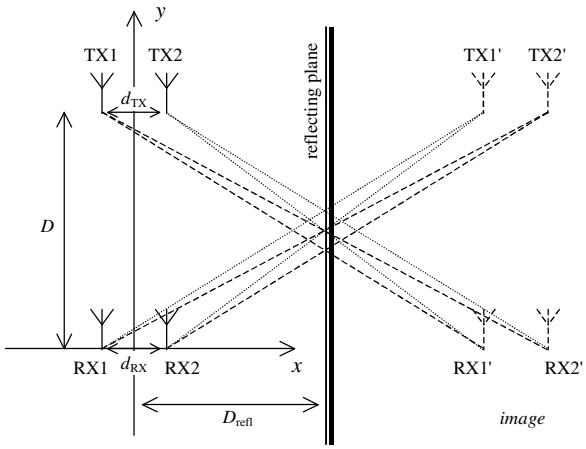


Figure 4: Antenna set-up with a reflecting plane. Only the extra paths that have to be taken into account in addition to the direct paths of Figure 2 are shown.

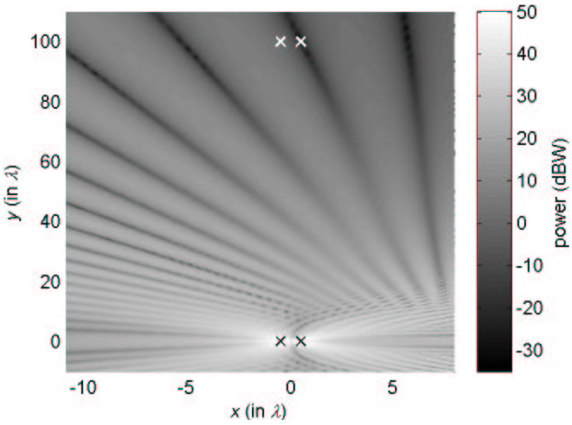


(a)

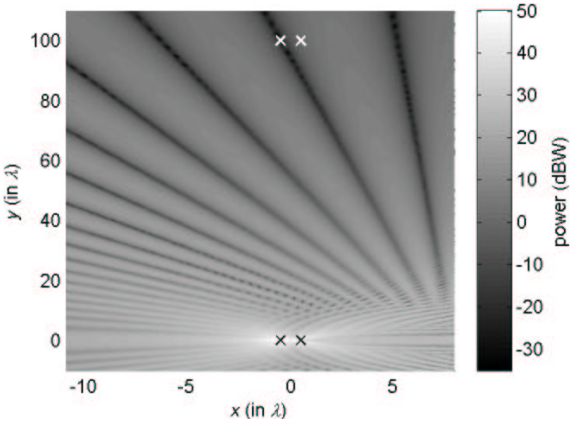


(b)

Figure 5: Antenna patterns after applying the first (a) and second (b) weight vector in a scenario with one reflecting plane at $x = 8\lambda$.

With the same parameters as in Section III, namely, $d_{TX} = 1\lambda$, $d_{RX} = 1\lambda$, $D = 100\lambda$ and $P_t = 0.035$ Watts, and with the extra information that $D_{refl}$ is chosen to be $8\lambda$, the channel matrix and the weight vectors can be determined. The antenna patterns after applying both weights are given in Figure 5. From these figures, we can see that the reflecting plane at $x = 8\lambda$ causes an interference pattern. Again, we see that applying the right weight suppresses the unwanted antenna.

## V. Two Reflecting Planes

In this scenario, we use the same parameters as the previous scenarios, except that we now assume that two ideal reflecting planes are present, one at $x = 8\lambda$, and one at $x = -6\lambda$. Since the two reflecting planes are parallel to each other, there will exist paths that only arrive at the receiver after a multiple of bounces between the two planes. Here, we will consider a maximum of one bounce and two bounces, respectively. The channel matrix and weight vectors can be determined for both cases following Section III and taking the ideal reflections into account. The antenna patterns after application of the weight vectors in case of a maximum of one and two bounces are shown, respectively, in Figure 6 and Figure 7.

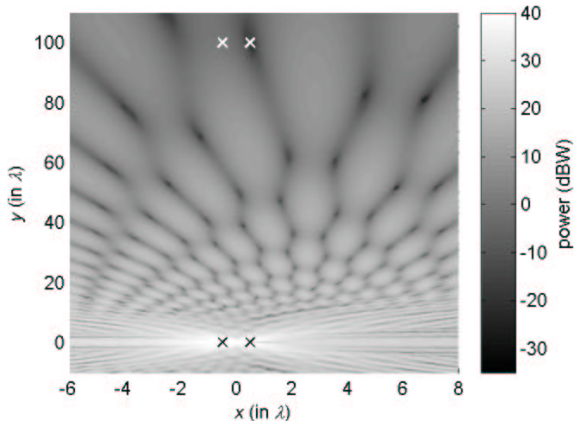


(a)

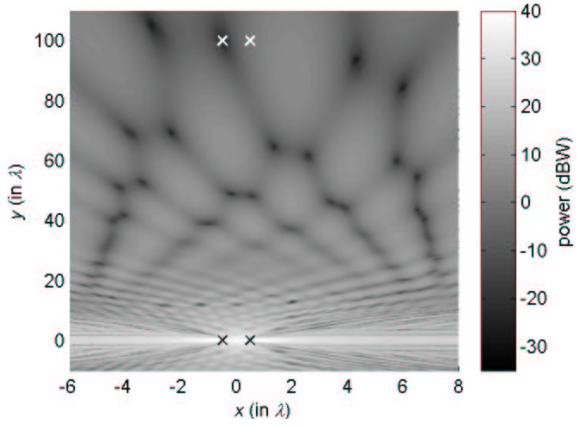


(b)

Figure 6: Antenna patterns after applying the first (a) and second (b) weight vector in a scenario with two reflecting planes (at $x = -6\lambda$ and $x = 8\lambda$), where only paths with a maximum of one bounce are taken into account.

From comparing the results of this figure with those of Figure 3, it becomes clear that the more reflections occur, the more chaotic the antenna patterns get. In Figure 6 and Figure 7, we can see that the undesired antenna is nulled with a spot, instead of with a beam (like in Figure 3), and that the desired antenna is (almost) located at a local maximum. This maximal separation between the wanted and unwanted antenna shows that the signals from both antennas can be treaded as uncorrelated (or independent). This observation speaks in favor of the robustness of MIMO systems in environments with many reflecting objects, i.e. *richly scattered* environments.

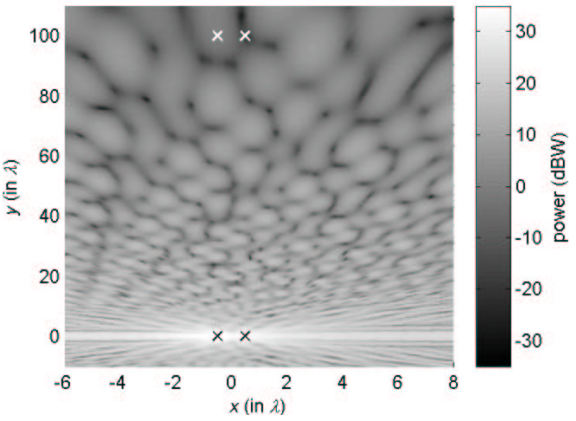


(a)

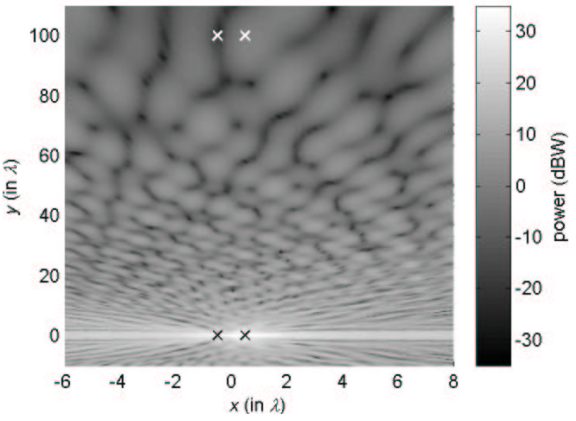


(b)

Figure 7: Antenna patterns after applying the first (a) and second (b) weight vector in a scenario with two reflecting planes (at $x = -6\lambda$ and $x = 8\lambda$), where only paths with a maximum of two bounces are taken into account.

## VI. Channel Estimation Errors

The observation of the previous section that MIMO is more robust in environments with many reflections can be confirmed by adding noise to the channel observation. In line with the previous sections, it is possible to illustrate how the antenna patterns are altered when the channel estimation is corrupted by noise. To include the influence of noise, we can add independent and identically distributed (i.i.d.) complex Gaussian noise to the four channel elements of the 2 ×

2 cases of the previous sections. With an average noise power of 10% of the average channel element power (i.e., the Signal-to-Noise Ratio (SNR) = 10 dB), and the assumption that the average channel element power is normalized to one, an example of the Additive White Gaussian Noise (AWGN) is given by

$$\begin{pmatrix} 0.0091 - j \cdot 0.0186 & -0.0826 - j \cdot 0.0933 \\ 0.0464 - j \cdot 0.0858 & -0.0326 + j \cdot 0.0658 \end{pmatrix}. \quad (8)$$

When adding this noise to the channel coefficients of the free space (pure LOS) case of Section III and applying correct scaling to maintain the SNR of 10 dB, the resulting antenna patterns after applying the weight vectors are given in Figure 8. Adding the same noise to the case with two reflecting planes where up to two bounces are considered (Section V), results in the antenna patterns of Figure 9.

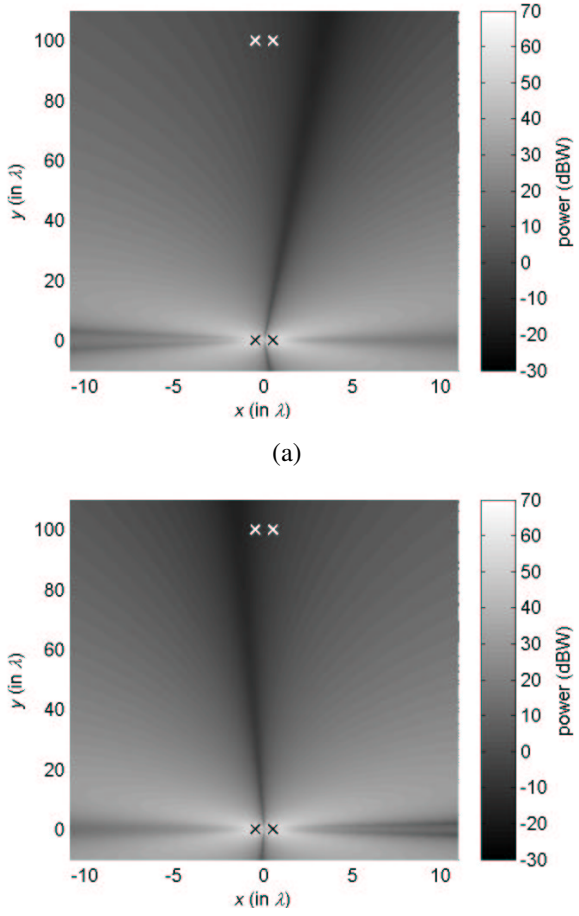


(a)

(b)

Figure 8: Antenna patterns after applying the first (a) and second (b) weight vector in free space with noise added to the channel observation.

When comparing the results of Figure 8 and Figure 9 with Figure 3 and Figure 7, respectively, we clearly see that the pure-LOS case strongly suffers from the additive noise. This can be explained by the fact that for this case the columns of the channel matrix have a strong resemblance (i.e., are highly correlated), resulting in a big error when noise is added. For the "richly scattered" case, the channel matrix is highly orthogonal and this property is hardly changed when noise is added. As a result, the antenna patterns for this case are barely altered. Similar results are achieved when other noise realizations are investigated, from which we can conclude that a MIMO system is indeed more robust in environments with many reflections.

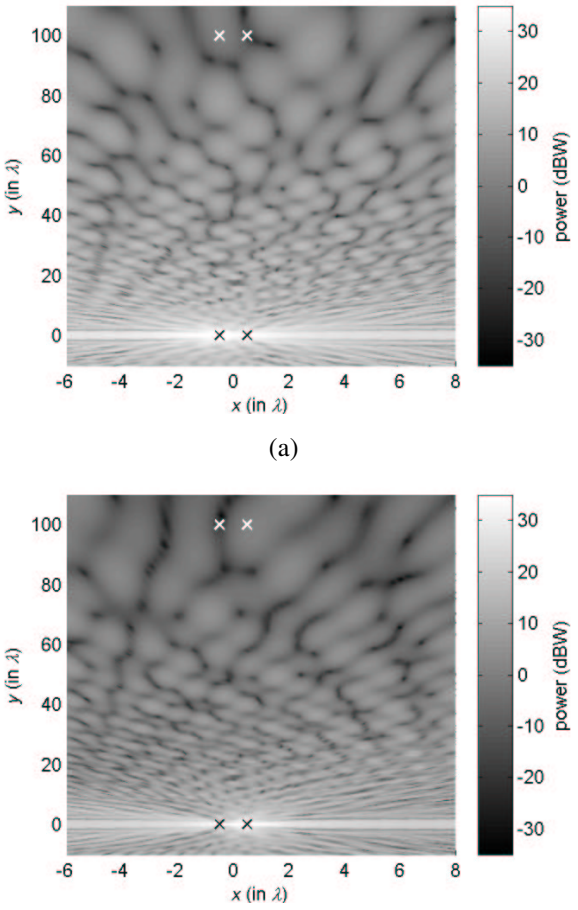


(a)

(b)

Figure 9: Antenna patterns after applying the first (a) and second (b) weight vector in a scenario with two reflecting planes (at $x = -6\lambda$ and $x = 8\lambda$), where only paths with up to two bounces are considered, and noise is added to the channel observation.

## VII. Conclusions

In this paper, we have seen that, for a communication system with multiple transmit and multiple receive antennas, the different signals from the different TX antennas (sent at the same frequency) can be separated at the receiver, under the assumption that the right weights can be found and applied. The ability of separating the different transmitter streams, results in a linear growth in throughput with the number of TX antennas, by which the potential capacity enhancement of MIMO is intuitively explained. Furthermore, for cases with many reflecting paths, it is shown that the undesired antenna is nulled

by a spot, whereas a local maximum is placed at the position of the desired antenna. This maximal separation between the two antennas speaks in favor of the robustness of MIMO systems in richly scattered environments.

## ACKNOWLEDGEMENT

The author would like to thank Xiao-Jiao Tao for the valuable discussions.

## REFERENCES

[1] G.J. Foschini and M.J. Gans, “On limits of wireless communications in a fading environment when using multiple antennas”, *Wireless Personal Communications*, vol. 6, no. 3, March 1998, pp. 311-335.

[2] Strang G., "Linear Algebra and its Applications", Third Edition, San Diego, Harcourt Brace Jovanovich, Publishers, 1988.

[3] Rappaport T.S., "Wireless Communications, Principles and Practice", New Jersey, Prentice-Hall, 1996.